

Swelling Kinetics and Rheological Behavior of Chitosan-PVA / Montmorillonite Hybrid Polymers

Nedjla Amri¹, Djamila Ghemati¹, Nadia Bouguettaya¹, Djamel Aliouche^{1*}

¹ Laboratory of Fibrous Polymers Treatment and Forming, F. S. I., M'Hamed Bougara University, Boumerdes 35000, Algeria

* Corresponding author, e-mail: aliouche.djamel@univ-boumerdes.dz

Received: 13 March 2018, Accepted: 12 June 2018, Published online: 02 August 2018

Abstract

This study involved preparation of hybrid polymer systems based on chitosan-poly(vinyl alcohol) (PVA) blends and modified Montmorillonite. These structures were characterized through microscopy and infrared spectroscopy; swelling measurements were performed to explore polymer absorbency. The behavior of polymer systems was studied through steady and oscillatory shear rheology. Results showed that more stable blend membranes were formed due to the strong interaction between chitosan and PVA. The membranes exhibited appreciable water uptake and were sensitive to saline solution with a slight shrinking.

Shear viscosity was described by Cross model to characterize non-Newtonian behavior of all polymer solutions, the shear thinning increases with PVA content, while viscosity increases with chitosan extent. In oscillatory experiments, it was observed that all measured viscoelastic properties were influenced by blends composition and clay content. For all samples, results show a typical behavior of an entangled system in the case of semi-dilute macromolecular viscoelastic fluids. The dynamic moduli exhibited higher values for blends, compared with values of neat polymers, which are an indication of a good stability and a tendency of gel formation. Therefore, the prepared chitosan-PVA systems, which exhibited high swelling degrees and suitable viscoelastic properties, have promising applications in tissue engineering and membrane processes.

Keywords

membrane, Na-MMT, swelling, viscosity, viscoelasticity

1 Introduction

Biopolymer membranes offer excellent biocompatibility and degradability; however, because of the significant sensitivity to water, their mechanical properties after swelling are poor. In order to reduce this weakness, the biopolymers used can be modified by physical blending [1], chemical grafting [2], crosslinking [3] and by formation of polymer-clay nanocomposites [4]. Polymer blending with distinctive molecular structures or different mechanical properties has become a technique of choice to produce materials with high characteristics. Blends of chitosan and poly(vinyl alcohol) (PVA) have been reported to provide suitable mechanical properties for drug release control [5], food packaging films [6] and liquid mixtures separation [7, 8]. These valuable properties are due to inter-molecular interactions between the blended polymers chains. However, most of the blend hydrogels are brittle and do not show high viscoelastic performance and thermal stability. To overcome these

intrinsic weaknesses, polymer based nanocomposites have been developed by dispersing fine ratio clay particles in the polymeric matrix [9]. The most widely used filler in such nanocomposites is Montmorillonite (MMT), a common clay mineral from the smectite family. Therefore, it is believed that well-combined nanocomposites of MMT and chitosan / PVA blends could find many potential applications, particularly in biomechanical engineering and membrane separation. Although characterization of bulk properties like swelling and diffusion rate is essential, most biomedical applications of blend polymers require a detailed perception of flow behavior and local mechanical properties. Understanding the polymer responsiveness to environmental changes is essential for the design of materials with suitable characteristics on macroscopic and microscopic scale. For this, rheological properties of polymer solutions need to be controlled in order to initiate steady and dynamic flow in favorable conditions.

Previously we have studied the flow properties of poly(acrylamide-co-acrylic acid) and poly(acrylamide-co-itaconic acid) hydrogel suspensions and related them to their swelling behavior [10, 11]. In order to explore the potential of chitosan / PVA blends as absorbent biomaterials, the present paper focuses on how addition of MMT fillers affects the swelling and rheological behavior of these polymers. Fourier transform infrared spectroscopy (FTIR) and scanning electron microscopy (SEM) were used to get information about the structural characteristics of the polymer nanocomposites. Effect of the blends composition and presence of fillers on the swelling of the prepared membranes was studied. Detailed rheological analysis was carried out to assess dynamic viscoelastic and steady flow properties of polymer solutions.

2 Experimental

2.1 Chemicals and Materials

PVA powder (Molecular weight 85.000-124.000 and 89 % hydrolyzed, Art. No. 363081) and Chitosan powder (Molecular weight of 190.000-300.000 and 85 % deacetylated, Art. No. 448877), were supplied by Sigma-Aldrich. Both powders were used without further purification. Acetic acid 99.8 % purity from Fluka Chemicals and NaCl from Panreac (Spain) were used as received. Deionized water was used for preparation of polymer solutions and in swelling experiments. The pristine clay used in this work was the Montmorillonite from Maghnia (west Algeria) purified by successive washings with deionized water; and the fraction with particle size smaller than 2 μm was obtained after careful aqueous decantation of the natural clay. The same fraction was then converted to Na-MMT form with dilute NaCl solution. Its cation exchange capacity was 90 meq / 100 g.

2.2 Preparation of polymer blends

Chitosan solution (2 % w/v) was prepared by dissolving chitosan in 1 % (v/v) aqueous acetic acid solution at room temperature under continuous stirring for overnight. PVA solution (5 % w/v) was prepared by dissolving the polymer powder in deionized water at 80 °C under stirring until complete dissolution had occurred (~ 4 h). Both polymer solutions were filtered using sintered glass, degassed in a vacuum and then carefully mixed at different weight ratios of Chitosan and PVA. The weight composition percentage chosen were 100/0 (chitosan), 70/30, 50/50, 30/70 (chitosan / PVA) and 0/100 (PVA). The mixtures were stirred for 24 h at room temperature to obtain homogeneous solutions.

2.3 Preparation of the nanocomposite polymers

For nanocomposites, suitable amount of sodium montmorillonite (Na-MMT) was dispersed in deionized water to form suspension of 5-wt% concentration with respect to the total mass of polymer. The clay suspension is sonicated for 120 min at room temperature and 37 kHz in an Elmasonic P bath (Schmidbauer GmbH, Germany). Next, the prepared suspension was added thoroughly to the previously prepared chitosan / PVA solutions and the mixtures were vigorously stirred for 24 h. In membranes preparation, the mixtures were poured into a petri-dish and allowed to dry at room temperature for 48 h. In the desiccator (silica gel replaced every 24 h); then further dried in vacuum for additional 24 h at 40 °C to remove the residue of water and acetic acid.

2.4 Measurements procedure

2.4.1 Characterization

- The microstructure of the membrane biopolymers was studied using a Philips XL 30 ESEM scanning electron microscope (SEM).
- The spectroscopic characterization of the membranes was performed by a Thermo Scientific Nicolet IS 10 Model Spectrophotometer equipped with ATR Thermo Scientific Smart iTR module. Analysis was carried out with 40 scans and 2 cm^{-1} of resolution, in the range of 4000-600 cm^{-1} .

2.4.2 Swelling measurements

The swelling behavior of the polymer membranes was examined in deionized water and saline solution at room temperature. For several applications, in particular in the medical and pharmaceutical fields, it is significant to know the behavior of absorbing materials in the physiological solution, usually simulated by aqueous 0.9 % NaCl solution. Prior to measurements, the membranes were cut into 5 \times 5 cm^2 and dried in a vacuum oven at 40 °C for 24 h to fix their dry weight (M_0). For the procedure, dried pre-weighed membranes were immersed into vials (500 mL) filled with deionized water (or saline) and removed at regular time-intervals, wiped superficially with filter paper to extract surface-bound water, weighed and then dipped in the same liquid. The mass swelling percentage was calculated from the following equation [12, 13]:

$$S_w (\%) = \frac{M_t - M_0}{M_0} \times 100 \quad (1)$$

where M_0 and M_t are initial dry mass and mass at different time-intervals, respectively. The amount of water absorbed

by the polymer membranes is characterized quantitatively by the equilibrium water content (EWC) which can be calculated using the following equation:

$$EWC(\%) = \frac{M_{\infty} - M_0}{M_{\infty}} \times 100 \quad (2)$$

M_0 and M_{∞} are the mass of dry gel and mass of swollen gel at equilibrium.

All the experiments were carried out in triplicate and the average values have been reported in the data.

2.4.3 Rheological Measurements

The rheological tests of polymer solutions were carried out under controlled shear rate mode, with AR-2000 Advanced Rheometer from T.A. Instruments (Newcastle, DE, USA), using a cone and plate sensor geometry (cone angle 2° , 40 mm diameter and $56 \mu\text{m}$ gap). The range of the shear rate for steady rate sweep test was from $0.1\text{--}400 \text{ s}^{-1}$. As the PVA solution is of very low consistency, flow curves were completed with a Couette fixture using a pair of coaxial cylinders with 15 mm of external diameter and gap of 2.5 mm. Silicone oil was added to the surface to prevent evaporation during measurements. For dynamic viscoelastic determination, the frequency spectra were conducted in the linear viscoelastic regime of the samples, as determined in preliminary tests by dynamic stress sweep measurements. The frequency sweeps were done over a range of $0.62\text{--}62.8 \text{ rad/s}$ ($0.1\text{--}10 \text{ Hz}$) at 20°C and constant oscillating stress amplitude.

3 Results and discussion

3.1 Characterization

- The polymer membranes prepared at different percentages of chitosan were studied by SEM. In Fig. 1, the SEM micrographs presented very similar morphological aspects for surfaces of PVA, chitosan and chitosan / PVA, showing the formation of uniform and continuous membranes. Nevertheless, some effect of phase separation was detected with droplet-like forms onto these Chitosan / PVA membranes after blending. Similar results were observed by E. S. Costa-Júnior et al. for Chitosan / PVA blends and attributed to chemical bonds effects [14]. Prior to blending, the macromolecular chains are mainly entangled in the polymer network; after mixing, PVA and chitosan develop physical and chemical bonds that are responsible of these droplet effects.

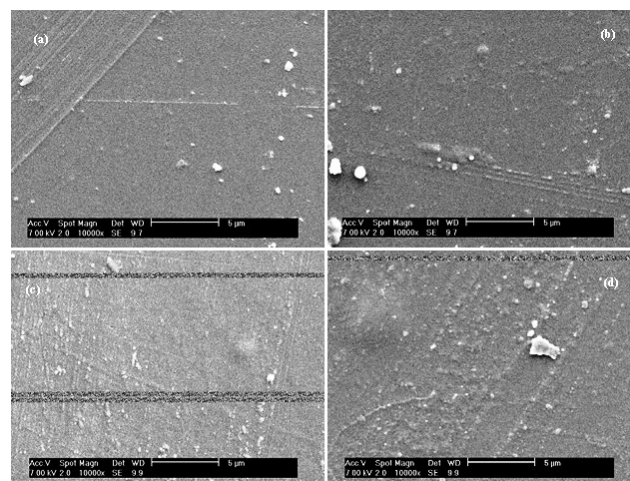


Fig. 1 SEM images of PVA (a); Chitosan (b); chitosan / PVA 30/70 (c) and chitosan / PVA 30/70 + 5 % Na-MMT (d).

- Spectroscopic analysis: FTIR spectroscopy is a useful technique for characterizing the specific intermolecular interactions between the chemical groups in polymer blends and for investigating the formation of associations from the blends with clay. These intermolecular interactions refer mainly to hydrogen bonding interactions; they result in either frequency shifting or band broadening of specific functional groups. Fig. 2 shows the FTIR spectra relative to the chitosan, PVA and Chitosan / PVA blends. For PVA (Fig. 3a) all major peaks related to hydroxyl and acetate groups were observed, the broad band detected between 3330 and 3230 cm^{-1} is associated with the stretching of O-H from the intermolecular and intramolecular hydrogen bonds [15]. The vibrational band at 2930 cm^{-1} is associated with the C-H stretching from alkyl groups. The peaks at 1725 cm^{-1} and 1088 cm^{-1} were due to the stretching C = O and C-O from acetate group. The characteristic bands of chitosan (Fig. 3e) were located at 3350 cm^{-1} for stretching band of OH group overlapping with N-H stretching band, and at 1635 cm^{-1} (NHCOCH_3), 1550 cm^{-1} ($-\text{NH}_2$ group), 1350 cm^{-1} (C-O stretching of primary alcohol groups) for amide I, amide II and amide III, respectively [16, 17]. The spectrum also shows peaks around 896 and 1146 cm^{-1} ($-\text{C}-\text{O}-\text{C}-$ glycoside links) corresponding to saccharide structure and peaks at 2800 and 2900 cm^{-1} are the typical C-H stretch vibrations. Spectra of Fig. 3(b), 3(c) and 3(d) show the absorption bands of the chitosan / PVA blends (30/70; 50/50; 70/30) respectively. As can be seen

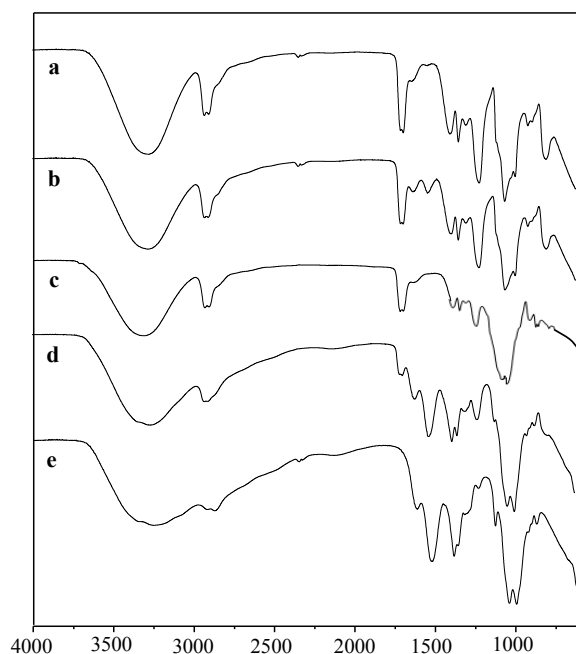


Fig. 2 FT-IR spectra of PVA (a); Chitosan / PVA blends [30/70 (b); 50/50 (c); 70/30 (d)] and Chitosan (e)

from the spectra, with increasing PVA content in the blended polymers, the absorption peaks at 1635 cm^{-1} (NHCOCH_3) and at about 1550 cm^{-1} for the $-\text{NH}_2$ group of chitosan decreased. The spectra region from 3200 cm^{-1} up to 3500 cm^{-1} was wider than pure PVA, mostly attributed to the overlapping signals from two groups: hydroxyls ($-\text{OH}$ in chitosan and PVA) and amino ($-\text{NH}$, chitosan). The association or dissociation of hydrogen bonding between these groups might cause such results [18].

Fig. 3 shows the FTIR spectra relative to change in polymer membranes filled with 5 % Na-MMT clay. In order to show the polymer-clay association, the spectra were focused on the region $1100\text{--}800\text{ cm}^{-1}$ characteristic of stretching and bending vibrations of layered silicates. Na-MMT spectrum (Fig. 3a) shows the vibration bands at 1480 cm^{-1} for H-O-H bending, a large band between 1094 and 1008 cm^{-1} characteristic for Si-O-Si stretching vibration of silicates, and finally bands at about 953 and 842 cm^{-1} for AlAlOH , AlFeOH and AlMgOH bending vibrations [19]. Spectra of Fig. 4(b), 4(c), 4(d), 4(e) and 4(f) show the absorption bands of the PVA / Na-MMT, blends of chitosan / PVA / Na-MMT and chitosan / Na-MMT respectively. The spectra show the combination of characteristic absorptions due to the polymers and MMT

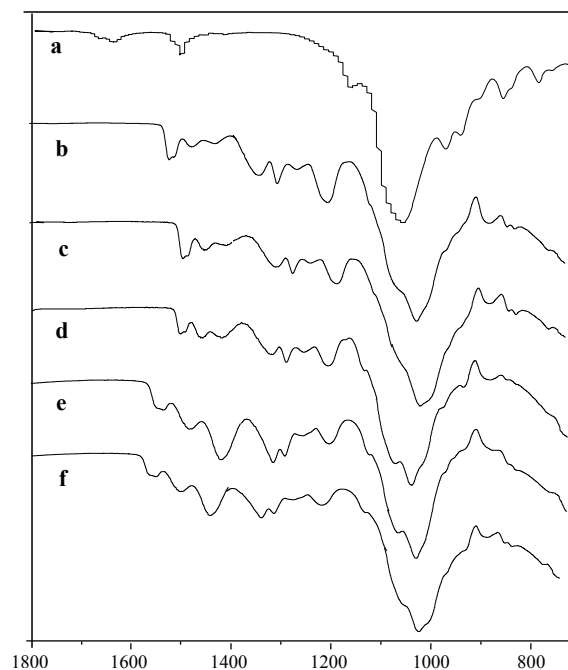


Fig. 3 FT-IR spectra of Na-MMT (a) and PVA (b), Chitosan / PVA blends [30/70 (c), 50/50 (d), 70/30 (e)], Chitosan (f) filled with 5 % Na-MMT.

groups. The peak at 1550 cm^{-1} of the $-\text{NH}_2$ group in the starting chitosan and chitosan / PVA (70/30) was shifted to 1508 cm^{-1} in the polymers / Na-MMT spectra, corresponding to the deformation vibration of the protonated amine group ($-\text{NH}_3^+$) of chitosan. This $-\text{NH}_3^+$ group interacts with the negatively charged sites of MMT [20]. The characteristic stretching band of Si-O appears clearly; it was shifted over the interval $1110\text{--}970\text{ cm}^{-1}$ for the filled polymers.

3.2 Swelling behavior

Polymers' swelling is governed by several parameters, which include presence of hydrophilic groups, properties of external solution and polymer network elasticity. The swelling is usually evaluated by the amount of liquid absorbed according to time up to saturation. Therefore, for polymer membranes the equilibrium swelling degree ($S_{w,\infty}$) is the most important parameter with respect to their biomedical applications where a fast and large water absorption capacity is required [21]. Based on experimental results, several authors have proposed a second-order kinetic equation to determine $S_{w,\infty}$ of polymer [22, 23]. Considering the second-order kinetics, the swelling rate at any time may be expressed as:

$$\frac{dS_w}{dt} = K(S_{w,\infty} - S_w)^2 \quad (3)$$

where S_{w_e} is determined by fitting S_w to time data for a second order equation of the form:

$$\frac{t}{S_w(t)} = \frac{1}{S_{w_e}} t + \frac{1}{K \cdot S_{w_e}^2} \quad (4)$$

where $S_w(t)$ is the polymer swelling at time t (min) and K ((g gel / g water) / min) is the second order swelling rate constant. All membranes exhibit a very fast response to liquids absorption and reach swelling equilibrium after 60 min; the equilibrium water contents (EWC), which ranged from 60 % to 72 %, were high. The values of swelling parameters are given in Table 1 for water absorption and Table 2 for saline solution. As seen from the value (~ 1) of the correlation coefficients, the second order kinetic equation follows quite well the experimental data for all membrane compositions, showing a swelling kinetics of the second-order for all samples. Swelling is produced by the osmotic pressure resulting from difference in

concentration of mobile ions between the internal polymer network and external solution. In addition, the behaviour of our blend membranes depends upon the composition of the polymer system, particularly when at least one constituent contains hydrophilic groups. In this case, the increase in hydrophilic polymer (PVA) within the matrix produces an enhancement in its swelling capacity due to increased chain relaxation as well as osmotic pressure. Moreover, due to its large number of hydroxyl groups, PVA is a more hydrophilic polymer than chitosan. This latter, in turn, contributes to reducing the membranes swelling due to intra- and inter-molecular hydrogen bonds established between the hydroxyl and acetate groups. Our membranes were prepared without any crosslinking and are physically entangled, therefore, the degree of swelling for blend membranes, which was higher than that of PVA and chitosan membranes, increased with increasing PVA content. This behavior has been observed by several authors and

Table 1 Swelling parameters of Chitosan / PVA membranes in deionized water

Polymers	Pristine polymers			
	S_{w_e} (%)	$K_{S_w} \cdot 10^{-2}$ (g/g)	EWC (%)	R^2
Chitosan	163.13	0.34	61.73	0.998
Chitosan / PVA 70/30	216.92	0.52	68.25	0.999
Chitosan / PVA 50/50	261.10	0.23	72.06	0.999
Chitosan / PVA 30/70	269.54	0.43	72.78	0.999
PVA	181.16	0.38	64.24	0.998
Polymers + 5 % Na-MMT				
Chitosan	138.12	0.32	57.65	0.998
Chitosan / PVA 70/30	148.81	0.23	63.96	0.999
Chitosan / PVA 50/50	181.16	0.23	57.65	0.999
Chitosan / PVA 30/70	257.73	0.12	69.36	0.998
PVA	157.98	0.19	58.93	0.998

Table 2 Swelling parameters of Chitosan / PVA membranes in saline solution (0.9 % NaCl)

Polymers	Pristine polymers		
	S_{w_e} (%)	$K_{S_w} \cdot 10^{-2}$ (g/g)	R^2
Chitosan	148.81	0.49	0.998
Chitosan / PVA 70/30	189.03	0.48	0.999
Chitosan / PVA 50/50	232.02	0.30	0.999
Chitosan / PVA 30/70	257.73	0.55	0.999
PVA	164.20	0.54	0.999
Blend polymers + 5 % Na-MMT			
Chitosan	132.80	0.49	0.998
Chitosan / PVA 70/30	145.14	1.05	0.999
Chitosan / PVA 50/50	166.11	0.79	0.999
Chitosan / PVA 30/70	256.41	0.17	0.999
PVA	146.84	0.79	0.998

attributed to the lower crystallization and less dense structure of the blends compared with Chitosan and PVA membranes [24, 25]. Moreover, as seen in Table 2, the swelling is reduced in presence of saline solution: this decrease results from the counter ions effect of Na^+ around the polymer, which induces a collapse of its internal network by a decrease of the osmotic pressure difference between the copolymer and the external solution when the ionic strength increases [26]. Both equilibrium swelling and water content (EWC) show similar decreasing trends in presence of filled membranes, this decrease can be interpreted by the fact that clay play a role of crosslinking agent for nanocomposite membranes, fixing and reducing polymer mobility, which resulted in a lower swelling rate [27]. The plasticizer effect of nanoparticles was reflected by acquiring a more compact polymer network.

3.3 Rheological analysis

3.3.1 Viscosity behavior of polymer solutions

Steady rate sweep test gives the shear viscosity of polymer solutions as a function of shear rate. The typical behavior of pseudoplastic fluid is confirmed for all samples as a function of increasing shear rate. The apparent viscosity of polymer solutions decreases gradually with increase in shear rate, and was a strong function of polymer composition; the zero-shear viscosity (η_0) increases with increasing chitosan content. This rise is due to the increase in intra-chains hydrophobic bonds in chitosan and intermolecular interactions between chitosan and PVA molecules, thus improving the H-bonding between the two polymers. At low shear rates, all polymer solutions show a higher viscosity, which decreases with increasing shear rate: in the low shear rate, the stretching polymer molecules intertwined to form aggregates, the high viscosity is due to large resistance against flow. Increasing shear rate destroys aggregates; macromolecules arrange along the flow direction, consequently the flow resistance declines resulting in a decrease of apparent viscosity. This shear-thinning behavior of polymer solutions is a consequence of the uncoiling and aligning of polymer chains when exposed to shear flow [28]. This effect is in agreement with behavior of biopolymer solutions, especially polysaccharides, which exhibit Newtonian flow at low-shear rates with a constant zero-shear viscosity (η_0) over a limited shear range that is followed by a shear-thinning range (non-Newtonian) where viscosity decreases in accordance with power law; and finally reaches a limiting and constant infinite-shear-viscosity (η_∞). Because most

biopolymer solutions show the well-known shear-thinning behavior, a number of rheological models can be used to describe the shear rate-apparent viscosity data. The Cross equation (5) for non-Newtonian fluids was developed based on the assumption that the pseudoplastic flow is related to the formation and rupture of structural linkages of the materials [29].

$$\eta = \eta_\infty + \frac{(\eta_0 - \eta_\infty)}{[1 + (\alpha_c \cdot \dot{\gamma})^m]} \quad (5)$$

In this model, η (Pa.s) is the apparent viscosity of polymer solution, $\dot{\gamma}$ the shear rate (s^{-1}), α_c (s) a time constant related to the relaxation time of the polymer and m is a dimensionless exponent indicating the viscosity degree dependence on shear rate in the shear-thinning region. A value of 0 for m implies a Newtonian behavior, with m tending to 1 for increasing shear-thinning behavior. PVA solution shows shear-thinning behavior but a Newtonian domain (η_∞) is reached at the highest shear rates, we tested the Cross model with four adjustable parameters, including the limiting viscosity at "infinite" shear rate (η_∞), this four-parameter model provided excellent fits to the data and η_∞ was easily measurable. The infinite shear viscosity values were: $\eta_\infty = 0.032 \pm 2.10^{-4}$ Pa.s for pure PVA, $\eta_\infty = 0.056 \pm 7.10^{-4}$ Pa.s for PVA + 5 % Na-MMT systems.

For chitosan and chitosan / PVA solutions, values of η_∞ are at a very low level and very difficult to determine experimentally. Despite the good fits to the data, the model gave negative values of η_∞ . At high shear rate, Newtonian viscosity was never approached; therefore, to avoid consequent errors in estimation of the other Cross parameters, η_∞ has been neglected for these polymer solutions [30]. Consequently, for our experimental data, considering that $\eta_\infty \ll \eta_{app}$, we used Cross model with three adjustable parameters, assuming $\eta_\infty = 0$ for chitosan and chitosan / PVA solutions [31, 32]. The flow parameters are shown in Table 3. For PVA the zero shear viscosity and Cross parameters decreased in presence of clay confirming the role of the Na-MMT as a plasticizer, the clay particles have caused the decrease in the resistance of polymer solutions against the flow. The polymeric chains entrapped between the clay layers are highly oriented and flow easily due to the loss of their entanglements with the neighboring chains. In these conditions, the local frictions decrease and thus facilitate the chain movements in the direction of flow. However, the plasticizer effect of clay gives a more compact hydrogel network with better mechanical and thermal properties. For Chitosan the increase in η_0 could

Table 3 Cross model data analysis for Chitosan, PVA and blends solutions

Nature of polymer solution	η_0 (Pa.s)	α_c (s)	m	R ²
Pristine polymer solutions				
Chitosan	$0.38 \pm 0.2 \cdot 10^{-3}$	$0.45 \cdot 10^{-2}$	$0.84 \pm 3.6 \cdot 10^{-3}$	0.999
Chitosan / PVA 70/30	$0.89 \pm 0.4 \cdot 10^{-3}$	$0.84 \cdot 10^{-2}$	$0.66 \pm 0.7 \cdot 10^{-3}$	0.999
Chitosan / PVA 50/50	$0.60 \pm 0.3 \cdot 10^{-3}$	$0.27 \cdot 10^{-2}$	$0.60 \pm 0.9 \cdot 10^{-3}$	0.999
Chitosan / PVA 30/70	$0.31 \pm 0.3 \cdot 10^{-3}$	$0.59 \cdot 10^{-2}$	$0.73 \pm 1.6 \cdot 10^{-3}$	0.999
PVA	$0.18 \pm 2.5 \cdot 10^{-3}$	3.51	$0.97 \pm 9.2 \cdot 10^{-3}$	0.999
Polymer solutions + 5 % Na-MMT				
Chitosan	$0.87 \pm 2.6 \cdot 10^{-3}$	$1.12 \cdot 10^{-2}$	$0.51 \pm 9.8 \cdot 10^{-3}$	0.997
Chitosan / PVA 70/30	$0.39 \pm 0.9 \cdot 10^{-3}$	$0.04 \cdot 10^{-2}$	$0.50 \pm 9.9 \cdot 10^{-3}$	0.991
Chitosan / PVA 50/50	$0.36 \pm 0.8 \cdot 10^{-3}$	$0.08 \cdot 10^{-2}$	$0.54 \pm 7.2 \cdot 10^{-3}$	0.993
Chitosan / PVA 30/70	$0.25 \pm 0.7 \cdot 10^{-3}$	$0.12 \cdot 10^{-2}$	$0.65 \pm 9.1 \cdot 10^{-3}$	0.991
PVA	$0.14 \pm 2.6 \cdot 10^{-3}$	2.08	$0.73 \pm 9.5 \cdot 10^{-3}$	0.996

be attributed to a more limited molecular motion because of the higher degree of entanglement usually found in solutions of this polysaccharide.

3.3.2 Dynamic shear of polymer solutions

The viscoelastic properties of polymer solutions were described in terms of two dynamic mechanical properties as a function of frequency (ω): elastic modulus, G' and viscous modulus, G'' . Another measure is the loss tangent, $\tan \delta$, which is defined as $\tan \delta = G'' / G'$, where δ is the phase angle between the viscous and elastic moduli during one deformation cycle. G' and G'' are usually determined as function of frequency at constant amplitude, in the linear viscoelastic range. In our experiments, the frequency sweeps were conducted over a range of 0.628–62.8 rad/s at a stress within the linear viscoelastic region as determined from the stress sweep curves. Fig. 4 and Fig. 5 show frequency sweeps for chitosan, PVA and chitosan / PVA blends solutions respectively. Figures plots display a typical behavior of an entangled system in the case of semi-dilute macromolecular viscoelastic fluid as expected: the spectra develop an increasingly elastic shape as frequency increases and observation time decreases [33]. Magnitude of G' and G'' increased slightly with increase of ω over the all range of frequency. For all samples G'' exceeds G' at low frequencies, and there is a crossover between the two moduli. Afterwards, at high frequency, G' become larger than G'' . At low frequencies the polymer solutions exhibited liquid-like behavior as expected ($G'' > G'$), after an initial lag time, both moduli increase, but G' increases faster than G'' . Gelation occurs when G' becomes higher than G'' in relation with the increasing number of physical

junctions responsible for the formation of polymer network. Thereafter, structure will behave predominantly as a more concentrated macromolecular solution; such behavior is typical of a weak macromolecular gel. In these "weak gels", there is a higher dependence on frequency for the dynamic moduli, suggesting the existence of relaxation processes

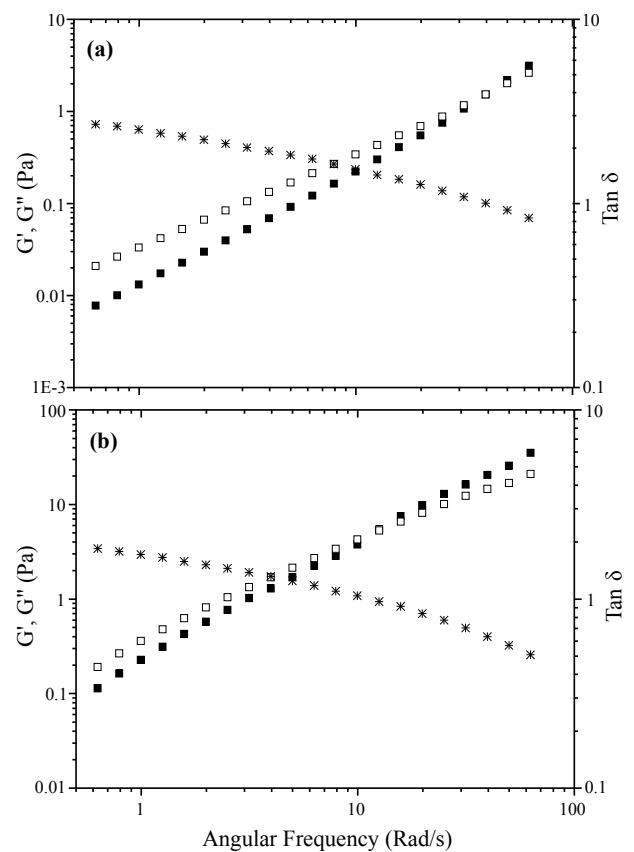


Fig. 4 Mechanical spectra of the PVA (a) and Chitosan (b) solutions: G' filled symbol, G'' open symbol

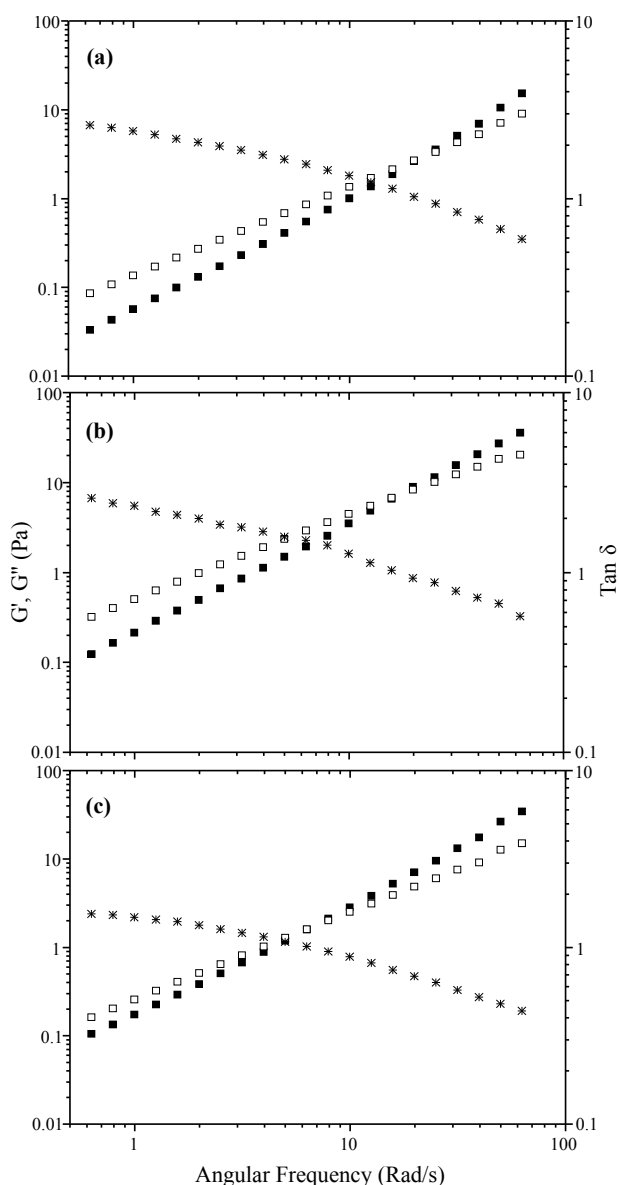


Fig. 5 Mechanical spectra of Chitosan / PVA blend solutions: 30/70 (a), 50/50 (b), 70/30 (c), (G' filled symbol, G'' open symbol)

occurring even at short time scales, and lower difference between moduli values, indicating that a lower percentage of the stored energy is recovered. On the other hand, for all samples, the polymer solutions become increasingly more viscoelastic as chitosan ratio is increased; as evidenced by the shift of the crossover point to lower frequencies.

The transition from the viscous to the predominant viscoelastic behavior occurs at a crossover frequency of 39.65 rad/s for PVA and 12.54 rad/s for chitosan. For the blend polymer solutions, the crossover occurs at 19.87, 15.78 and 6.28 rad/s for chitosan / PVA with 30/70, 50/50 and 70/30 composition respectively. As expected these crossover frequencies correspond to very short characteristic relaxation

times ($t = 2\pi / \omega$ at $G' = G''$) ranging from 0.1 to 1 s indicating the onset of the growth of interconnected networks within the polymer solutions. The crossover frequency decreases as chitosan concentration increases because of increasing relaxation times. Moreover, the dynamic moduli exhibited higher values for blends compared to values of PVA; this fact is an indication of a good stability and a tendency of gel formation. The blends showed viscoelastic behavior of a predominantly gel character, becoming more compact with increasing chitosan content. As known, the storage modulus (G') can be considered as a measure of the extent of gel network formation, i.e. the higher G' value means the stronger gel intensity. The effect of chitosan or PVA content on the gelation process indicates that when chitosan content is increased, the gel intensity is enhanced. Conversely, for an increase of PVA content in the given blend solution, the value of storage moduli (G') was seen to decrease, i.e., viscoelasticity is reduced in favor of viscosity. These results are consistent with the gel mechanism: chitosan is responsible for the hydrophobic interactions, the increase in chitosan lead to intensification of the chains entanglements, which in turn increase gel intensity. PVA content is related to hydrogen-bonding interactions; with higher PVA content, longer gel time is needed to produce enough energy in order to reduce the hydrogen bonds and promote gel formation. Such results confirm those described by Tang et al. for blend of Chitosan / PVA [34]. These observations were further evidenced by the decrease in $\tan \delta$ for all polymer solutions, indicating the shift of the materials towards increased elasticity as frequency and chitosan amount increased. For all samples, $\tan \delta$ was seen to decrease: to 0.83 for PVA and to 0.51 for chitosan; for the blends $\tan \delta$ decreases to 0.59, 0.57 and 0.54 for the 30/70, 50/50 and 70/30 Chitosan / PVA solutions respectively. The influence of clay on the dynamic behavior of the polymers is illustrated in Fig. 6. The figure depicts frequency sweeps for Chitosan, PVA and Chitosan / PVA blends (Fig. 6a) and same polymers filled with 5 % Na-MMT clay (Fig. 6b), the data have been vertically shifted by 10^a with the given a ($a = 0, 1, 2, 3, 4$), to avoid overlapping. As seen in the plots the dynamic behavior of polymer nanocomposites is similar to that of neat polymers. However, addition of clay into polymers results in an increase in the interparticle interactions, weakly at first and then rather strongly as the clay concentration becomes higher and higher, in these conditions the dynamic moduli of nanocomposites exhibit higher values than neat polymers. Interestingly, addition of clay particles into these polymer solutions leads to a

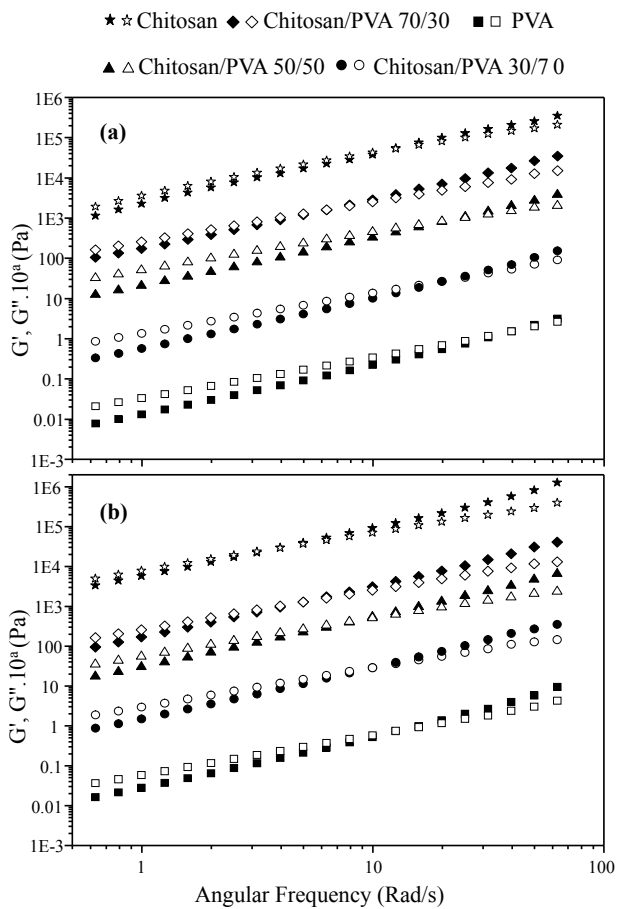


Fig. 6 Variation of loss and storage moduli as a function of frequency for the PVA / Chitosan solutions: (a) Pure polymers; (b) Polymers + 5 % Na-MMT. To avoid overlapping, the data have been vertically shifted by 10a with a = 0, 1, 2, 3, 4.

decrease in $\tan \delta$, indicating that the elastic properties are raised more strongly than the viscous properties with polymers / Na-MMT. In presence of clay, values of $\tan \delta$ were decreased from 0.83 to 0.45 for PVA, and from 0.51 to 0.31 for chitosan. For polymer blends $\tan \delta$ was seen to decrease from 0.59 to 0.41 for 30/70 Cs / PVA; from 0.57 to 0.36 for 50/50 Cs / PVA; and finally from 0.54 to 0.32 for 70/30 Cs / PVA respectively. For these entanglement networks at low frequency the relaxation critical exponent n at critical gel point was determined using the Winter and Chambon criterion ($G' \sim \omega^2$ and $G'' \sim \omega$) from the power dependence between dynamic moduli and ω [35]. Addition of Na-MMT produces pseudo-solid-like behavior and slower relaxation behavior of polymers. For all samples, the dependence of dynamic moduli on ω shows nonterminal behavior with power law dependence of G' and G'' . For G' the values of n are lower than that predicted from the Winter and Chambon criterion ($n \sim 1.2 - 1.7$), while for the loss modulus (G'') the values remain rather constant

close to 1 ($n \sim 0.86 - 1.1$). Furthermore, the value of n was reduced with increasing chitosan concentration; this decrease of n was attributed to entanglement effects [36].

4 Conclusion

A suitable polymer system for biomaterial use in membrane separation and biomechanical engineering was successfully prepared by physical blending and incorporating Na-MMT clay particles; this system was achieved through hydrogen bonds between PVA and chitosan, and hydrophobic interactions of chitosan chains. FTIR spectroscopy clearly shows that all spectra of polymer nanocomposites exhibit the presence of characteristic related absorptions due to the organic and inorganic groups, i.e. the characteristic stretching band of Si-O appears clearly in the nanocomposite material. Chitosan / PVA and Chitosan / PVA / Na-MMT systems have been showed significant absorption capacity. However, this swelling has been reduced in presence of clay due to their plasticizer effect. In steady and dynamic shear, these polymer systems exhibit an effective variety of rheological properties. The shear flow measurements showed that the zero shear viscosity is influenced by polymer composition and incorporation of clay particles. The shear thinning behavior increases with increased PVA concentration, polymers viscosity increases with chitosan concentration, as expected. The data were analyzed by using conventional flow Cross equation known as the model describing the flow behavior of the polymer solutions very well. The model was more satisfactory to describe the flow behavior of chitosan, PVA and chitosan / PVA blends with good fits to the data. Viscoelastic properties were investigated using oscillatory deformation tests. It was observed that all measured viscoelastic properties, including G' , G'' , and $\tan \delta$, were influenced by polymers composition and presence of clay. With increase in chitosan amount, the gel intensity is enhanced. Conversely, the PVA content is related to the hydrogen-bonding interactions: higher PVA content promote viscosity at the expense of elasticity. In presence of fillers, the dynamic moduli of all polymer nanocomposites exhibit higher values than neat polymers indicating that elastic properties are raised more strongly than viscous. The study advised that these polymer systems showed high swelling degrees and suitable viscoelastic properties, suggesting their application in biotechnology as membrane separation processes. Because of their biocompatibility and high water content, surface of the prepared polymer systems is highly hydrophilic and able to simulate some properties as of natural tissues.

References

- [1] Koyano, T., Koshizaki, N., Umehara, H., Nagura, M., Minoura, N. "Surface states of PVA / chitosan blended hydrogels", *Polymer*, 41(12), pp. 4461–4465, 2000.
[https://doi.org/10.1016/S0032-3861\(99\)00675-8](https://doi.org/10.1016/S0032-3861(99)00675-8)
- [2] Sokker, H. H., Abdel Ghaffar, A. M., Gad, Y. H., Aly, A. S. "Synthesis and characterization of hydrogels based on grafted chitosan for the controlled drug release", *Carbohydrate Polymers*, 75(2), pp. 222–229, 2009.
<https://doi.org/10.1016/j.carbpol.2008.06.015>
- [3] Liang, S., Liu, L., Huang, Q., Yam, K. L. "Preparation of single or double-network chitosan / poly(vinyl alcohol) gel films through selectively cross-linking method", *Carbohydrate Polymers*, 77(4), pp. 718–724, 2009.
<https://doi.org/10.1016/j.carbpol.2009.02.007>
- [4] Pavlidou, S., Papaspyrides, C. D. "A review on polymer-layered silicate nanocomposites", *Progress in Polymer Science*, 33(12), pp. 1119–1198, 2008.
<https://doi.org/10.1016/j.progpolymsci.2008.07.008>
- [5] Wang, Q., Du, Y.-M., Fan, L.-H. "Properties of chitosan / poly(vinyl alcohol) films for drug-controlled release", *Journal of Applied Polymer Science*, 96(3), pp. 808–813, 2005.
<https://doi.org/10.1002/app.21518>
- [6] Srinivasa, P. C., Ramesh, M. N., Kumar, K. R., Tharanathan, R. N. "Properties and sorption studies of chitosan-poly(vinyl alcohol) blend films", *Carbohydrate Polymers*, 53(4), pp. 431–438, 2003.
[https://doi.org/10.1016/S0144-8617\(03\)00105-X](https://doi.org/10.1016/S0144-8617(03)00105-X)
- [7] Lu, L., Peng, F., Jiang, Z., Wang, J. "Poly(vinyl alcohol) / Chitosan Blend Membranes for Pervaporation of Benzene / Cyclohexane Mixtures", *Journal of Applied Polymer Science*, 101(1), pp. 167–173, 2006.
<https://doi.org/10.1002/app.23158>
- [8] Svang-Ariyaskul, A., Huang, R. Y. M., Douglas, P. L., Pal, R., Feng, X., Chen, P., Liu, L. "Blended chitosan and polyvinyl alcohol membranes for the pervaporation dehydration of isopropanol". *Journal of Membrane Science*, 280(1-2), pp. 815–823, 2006.
<https://doi.org/10.1016/j.memsci.2006.03.001>
- [9] Strawhecker, K. E., Manias, E. "Structure and Properties of Poly(vinyl alcohol) / Na⁺ Montmorillonite Nanocomposites", *Chemistry of Materials*, 12(10), pp. 2943–2949, 2000.
<https://doi.org/10.1021/cm000506g>
- [10] Seddiki, N., Aliouche, D. "Synthesis, characterization and rheological behavior of pH sensitive poly(acrylamide-co-acrylic acid) hydrogels", *Arabian Journal of Chemistry*, 10(4), pp. 539–547, 2017.
<https://doi.org/10.1016/j.arabjc.2013.11.027>
- [11] Angar, N.-E., Aliouche, D. "Rheological Behavior and Reversible Swelling of pH Sensitive Poly(acrylamide-co-itaconic acid) Hydrogels", *Polymer Science, Series A*, 58(4), pp. 541–549, 2016.
<https://doi.org/10.1134/S0965545X16040015>
- [12] Gudeman, L. F., Peppas, N. A. "Preparation and characterization of pH-sensitive, interpenetrating networks of poly(vinyl alcohol) and poly(acrylic acid)", *Journal of Applied Polymer Science*, 55(6), pp. 919–928, 1995.
<https://doi.org/10.1002/app.1995.070550610>
- [13] Karadag, E., Saraydin, D., Güven, O. "A study on the adsorption of some cationic dyes onto acrylamide / itaconic acid hydrogels", *Polymer Bulletin*, 36(6), pp. 745–752, 1996.
<https://doi.org/10.1007/BF00338639>
- [14] Costa-Júnior, E. S., Barbosa-Stancioli, E. F., Mansur, A. A. P., Vasconcelos, W. L., Mansur, H. S. "Preparation and characterization of chitosan / poly(vinyl alcohol) chemically crosslinked blends for biomedical applications", *Carbohydrate Polymers*, 76(3), pp. 472–481, 2009.
<https://doi.org/10.1016/j.carbpol.2008.11.015>
- [15] Ahmad, A. L., Ooi, B. S. "Properties-performance of thin film composites membrane: study on trimesoyl chloride content and polymerization time", *Journal of Membrane Science*, 255(1-2), pp. 67–77, 2005.
<https://doi.org/10.1016/j.memsci.2005.01.021>
- [16] Nam, S. Y., Lee, Y. M. "Pervaporation and properties of chitosan-poly(acrylic acid) complex membranes", *Journal of Membrane Science*, 135(2), pp. 161–171, 1997.
[https://doi.org/10.1016/S0376-7388\(97\)00144-0](https://doi.org/10.1016/S0376-7388(97)00144-0)
- [17] Cui, Z., Xiang, Y., Si, J., Yang, M., Zhang, Q., Zhang, T. "Ionic interactions between sulfuric acid and chitosan membranes", *Carbohydrate Polymers*, 73(1), pp. 111–116, 2008.
<https://doi.org/10.1016/j.carbpol.2007.11.009>
- [18] Lu, L., Peng, F., Jiang, Z., Wang, J. "Poly(vinyl alcohol) / Chitosan Blend Membranes for Pervaporation of Benzene / Cyclohexane Mixtures", *Journal of Applied Polymer Science*, 101(1), pp. 167–173, 2006.
<https://doi.org/10.1002/app.23158>
- [19] Madejová, J. "FTIR techniques in clay mineral studies", *Vibrational Spectroscopy*, 31(1), pp. 1–10, 2003.
[https://doi.org/10.1016/S0924-2031\(02\)00065-6](https://doi.org/10.1016/S0924-2031(02)00065-6)
- [20] Monvisade, P., Siriphannon, P. "Chitosan intercalated montmorillonite: Preparation, characterization and cationic dye adsorption", *Applied Clay Science*, 42(3-4), pp. 427–431, 2009.
<https://doi.org/10.1016/j.clay.2008.04.013>
- [21] Tokarev, I., Minko, S. "Stimuli-responsive hydrogel thin films", *Soft Matter*, 5(3), pp. 511–524, 2009.
<https://doi.org/10.1039/B813827C>
- [22] Schott, H. "Swelling kinetics of polymers", *Journal of Macromolecular Science, Part B, Physics*, 31(1), pp. 1–9, 1992.
<https://doi.org/10.1080/00222349208215453>
- [23] Vallés, E., Durando, D., Katime, I., Mendizábal, E., Puig, J. E. "Equilibrium swelling and mechanical properties of hydrogels of acrylamide and itaconic acid or its esters", *Polymer Bulletin*, 44(1), pp. 109–114, 2000.
<https://doi.org/10.1007/s002890050580>
- [24] Zheng, H., Du, Y., Yu, J., Huang, R., Zhang, L. "Preparation and Characterization of Chitosan / Poly(vinyl alcohol) Blend Fibers", *Journal of Applied Polymer Science*, 80(13), pp. 2558–2565, 2001.
<https://doi.org/10.1002/app.1365>
- [25] Zhang, Y., Huang, X., Duan, B., Wu, L., Li, S., Yuan, X. "Preparation of electrospun chitosan / poly(vinyl alcohol) membranes", *Colloid and Polymer Science*, 285(8), pp. 855–863, 2007.
<https://doi.org/10.1007/s00396-006-1630-4>

- [26] Nguyen, N.-T., Liu, J.-H. "Fabrication and characterization of poly(vinyl alcohol) / chitosan hydrogel thin films via UV irradiation", *European Polymer Journal*, 49(12), pp. 4201–4211, 2013.
<https://doi.org/10.1016/j.eurpolymj.2013.09.032>
- [27] Kokabi, M., Sirousazar, M., Hassan, Z. M. "PVA–clay nanocomposite hydrogels for wound dressing", *European Polymer Journal*, 43(3), pp. 773–781, 2007.
<https://doi.org/10.1016/j.eurpolymj.2006.11.030>
- [28] Clasen, C., Kulicke, W.-M. "Determination of viscoelastic and rheo-optical material functions of water-soluble cellulose derivatives", *Progress in Polymer Science*, 26(9), pp. 1839–1919, 2001.
[https://doi.org/10.1016/S0079-6700\(01\)00024-7](https://doi.org/10.1016/S0079-6700(01)00024-7)
- [29] Cross, M. M. "Rheology of non-Newtonian fluids: A new flow equation for pseudoplastic systems", *Journal of Colloid Science*, 20(5), pp. 417–437, 1965.
[https://doi.org/10.1016/0095-8522\(65\)90022-X](https://doi.org/10.1016/0095-8522(65)90022-X)
- [30] Rao, M. A. "Rheology of Food Gum and Starch Dispersions", In: *Rheology of Fluid, Semisolid, and Solid Foods*. Food Engineering Series, Springer, Boston, Massachusetts, USA, 2014, pp. 161–229.
https://doi.org/10.1007/978-1-4614-9230-6_4
- [31] Lopes da Silva, J. A., Gonçalves, M. P., Rao, M. A. "Rheological Properties of High-Methoxyl Pectin and Locust Bean Gum Solutions in Steady Shear", *Journal of Food Science*, 57(2), pp. 443–448, 1992.
<https://doi.org/10.1111/j.1365-2621.1992.tb05513.x>
- [32] Abdel-Khalik, S. I., Hassager, O., Bird, R. B. "Prediction of Melt Elasticity from Viscosity Data", *Polymer Engineering and Science*, 14(12), pp. 859–867, 1974.
<https://doi.org/10.1002/pen.760141209>
- [33] Giboreau, A., Cuvelier, G., Launay, B. "Rheological behavior of three biopolymer / water systems with emphasis on yield stress and viscoelastic properties", *Journal of Texture Studies*, 25(2), pp. 119–137, 1994.
<https://doi.org/10.1111/j.1745-4603.1994.tb01321.x>
- [34] Tang, Y.-F., Du, Y.-M., Hu, X.-W., Shi, X.-W., Kennedy, J. F., "Rheological characterization of a novel thermosensitive chitosan / poly(vinyl alcohol) blend hydrogel", *Carbohydrate Polymers*, 67(4), pp. 491–499, 2007.
<https://doi.org/10.1016/j.carbpol.2006.06.015>
- [35] Winter, H. H., Chambon, F. "Analysis of Linear Viscoelasticity of a Crosslinking Polymer at the Gel Point", *Journal of Rheology*, 30(2), pp. 367–382, 1986.
<https://doi.org/10.1122/1.549853>
- [36] Kjøniksen, A.-L., Nyström, B. "Effects of Polymer Concentration and Cross-Linking Density on Rheology of Chemically Cross-Linked Poly(vinyl alcohol) near the Gelation Threshold", *Macromolecules*, 29(15), pp. 5215–5222, 1996.
<https://doi.org/10.1021/ma960094q>